A Framework for Assessing Structural Resilience of Offshore Wind Turbines

David Wilkie
Graduate Student, Dept. of Civil, Environmental, and Geomatic Engineering, University College London, London, UK

Carmine Galasso
Associate Professor, Dept. of Civil, Environmental, and Geomatic Engineering, University College London, London, UK

ABSTRACT: The concept of resilience provides a useful framework for considering an offshore wind turbine (OWT) as a system of integrated structural and mechanical components. This paper proposes quantifying economic losses associated with failure of an OWT using a catastrophe (CAT) risk modelling framework. Providing a first step towards evaluating offshore wind farm (OWF) resilience. A site-specific assessment of structural fragility is developed and then combined with empirical mechanical and electrical component failure rates to assess losses. The results from a case-study application indicate that failure of the structure plays a major role on the overall risk profile of an OWF, but depends on the severity of the site environmental conditions.

1. INTRODUCTION

The offshore wind industry has grown to the point where it supplies 12.6GW of electricity within Europe, with a further 24.6GW worth of projects due to be installed by 2020. Historically, this form of energy production has been expensive; however, the overall cost of recent offshore wind farms (OWFs) have fallen, due to reductions in the cost of debt financing. However, cost saving remains an important objective for operators who have to enter competitive bids for potential OWF sites.

A recent UK government report (Arwas and Charlesworth 2012) highlighted that "integrated design" could significantly contribute to cost reduction. Offshore wind turbines (OWTs) are unique engineering structures that rely on both electrical and mechanical components (e.g., generator and gearbox) and structural components (e.g., tower, monopile, transition piece, and blades). One challenge in "integrated design" is dealing with uncertainty in environmental conditions during extreme events (e.g., severe windstorm), and other uncertainties relating to the structural response and capacity. Quantifying the failure of these diverse sub-systems to assess the impact on the OWT and OWF represents a major challenge.

2. STRUCTURAL RESILIENCE OF OWTS

The concept of structural resilience provides a useful framework to enact integrated design, allowing the rational assessment of a system performance in the presence of uncertainties. The term has been applied in several different fields and has many overlapping definitions summarized by (Hosseini et al. 2016). However, one possible definition suitable for application to structural systems characterizes resilience through quantitative metrics. According to this definition, resilience can be schematically described by Figure 1. The solid line indicates the system performance (e.g., electricity generation) which is reduced after a disruptive event (e.g., a windstorm) occurring at t_0 and gradually recovers along the time axis, to different performance levels. In this context, resilience is quantified as the shaded area below the functionality curve and is determined by the following four metrics characterizing the system:

- *Robustness* – The capability of the system to withstand a disruptive event. It can be quantified as the residual functionality directly after the event and it is therefore a measure of overall system performance.
- *Rapidity* – The speed to recover, contain losses, and avoid disruptions. It can be viewed as the rate of recovery, i.e., the slope of recovery in Figure 1, and therefore determines the time gap between t_0 and a recovered state.
- *Redundancy* – The extent to which other components can be substituted after a disruptive event.
- *Resourcefulness* – The capacity to diagnose and prioritize problems that can cause reduced functionality, then to initiate measures that will lead to functional recovery. Relates to the ability of an organization to react after an event and therefore influences the rapidity.

It may be difficult to quantify some of these properties, especially at the design stage. For instance, information regarding the capacity of an organization to make budget available after a disruptive event, part of resourcefulness, is seldom available to the designer. Nor would it be clear to the designer whether an operator would decide to restore functionality to the original or a degraded level (t_D in Figure 1). Therefore, a methodology for assessing structural resilience of OWTs that relies on the robustness and redundancy of the structure would allow the concept to be applied directly at the design stage. An approach, investigated by (Bruneau and Reinhorn 2007), assumes that the loss of functionality after a disruptive event and the time to recovery are correlated. Similarly (Quiel et al. 2015) defined a relative resilience indicator (RRI), which is correlated to the resilience (R) of structures exposed to blast loading:

$$R(E) \propto RRI(E) = 1/C(E) \qquad (1)$$

In Eq. (1), RRI can be defined as the inverse of the consequence (C) of a disruptive event (E). Under this assumption, a structure experiencing a lower consequence (i.e., less damage and lower economic loss) as the result of a hazardous event, is viewed as more resilient. This approach is suitable for application to OWTs, using economic losses (e.g., repair costs) as a metric which represents the effect of failure. This concept could be extended to include downtime, through financial loss due to business interruption.

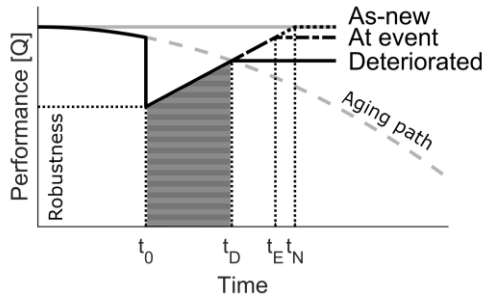

Figure 1. Graphical definition of resilience after an event (at t_0), with different repair options.

3. CATASTROPHE RISK MODELLING FRAMEWORK FOR OWTS

A framework based on Catastrophe (CAT) risk modelling is proposed, to assess structural and non-structural risk associated with OWTs exposed to extreme conditions. It is based on downgrading risk into conditional probability distributions which are evaluated independently and sequentially, and finally combined using the law of total probability. This approach allows expected loss of a system ($E(\mathrm{L})$) to be computed, in terms of conditional probability density functions (PDF) ($f[\cdot \mid \cdot]$):

$$E(L) = \int\int E[L|DM] \cdot f[DM|IM] \cdot f[IM] \cdot dDM \cdot dIM \qquad (2)$$

In Eq. (2), the main interface variables are: a measure of the intensity of a natural hazard (intensity measure; or IM), e.g., wind speed or wave height and damage measures (DMs), e.g., the physical condition of the structure and/or its components as a function of the IM. The framework is specifically tailored here to OWTs and can be expressed through a flowchart (Figure 2) for a specific OWT that consists of both

structural and mechanical / electrical components. The individual components of the framework are described in more detail in the following sections.

The structural and equipment components are treated differently in the proposed framework. Structural failure is predicted analytically, using site-specific environmental conditions, whereas equipment failure data typically comes from empirical databases which record rates of failure, but not environmental conditions.

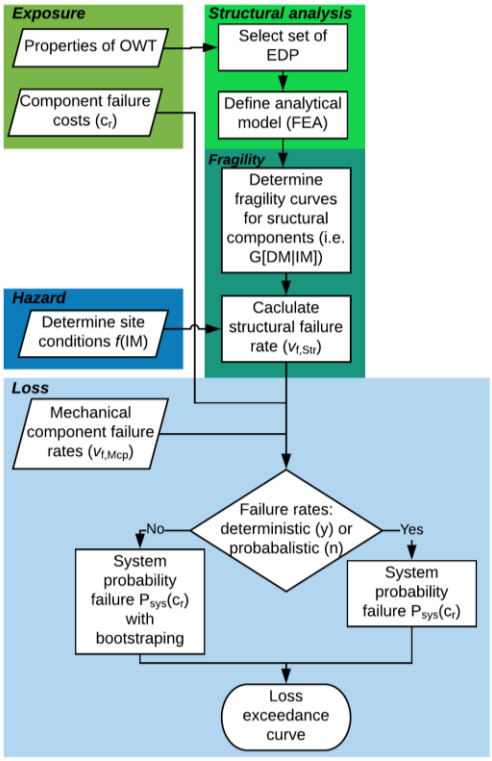

Figure 2: Proposed framework for OWF loss assessment.

3.1. Hazard

The primary environmental hazards threatening OWTs are those relating to severe wind or wave conditions. The conditions are frequently parameterized using separate variables, common choices are the significant waves height (Vorpahl et al. 2013) and the 10-minute mean wind speed. These can be combined into a single IM, assuming that wind and waves are linked by the mean return period (MRP), i.e., assuming the most extreme conditions associated with each MRP are coincident, a conservative, yet practical assumption to assess OWTs (e.g., Wei et al. 2014). Specific values of mean wind speed and significant wave height can be calculated using an appropriate probabilistic model, which describes frequency of occurrence of the environmental conditions at a site. Seismic hazards are also relevant for some OWF sites, but are not relevant for the specific location considered in this study.

3.2. Exposure

The structural response of an OWT is highly dependent on turbine specific parameters including the power rating (i.e., the power output) and control system (Vorpahl et al. 2013). Exposure data for an OWT should include all pertinent information required for loss assessment, including: location, geometrical properties, material properties and repair cost for all OWT components.

3.3. Structural analysis

A numerical model, to be solved using finite-element analysis, is typically used to predict structural response to environmental conditions represented through the selected IMs. For an OWT exposed to stochastic environmental loading, the use of dynamic time-history analysis is a common approach (Vorpahl et al. 2013). A key element of this process consists of specifying a set of limit states defining its performance criteria. In the ultimate limit state (ULS), for instance, failure of an OWT relates to the exceedance of the structure load-carrying capacity. All structural components are exposed to this form of failure and should therefore be assessed by an analytical model.

3.4. Fragility

Fragility functions express the probability that a damage state occurs given a level of hazard intensity (IM) as a conditional cumulative distribution function (CDF), $G[\mathrm{DM}|\mathrm{IM}]$. The structural analysis model is typically used to estimate the probability of failure conditional on the IM. This is achieved by running simulations repeatedly over a set of IMs, resulting in a set of outputs corresponding to each model and IM realization. The probability of failure is the mean number of failures at each IM and can be expressed

as a functional relationship by fitting a parametric distribution (typically lognormal) or directly using output from structural analysis to generate an empirical fragility curve (e.g., Iervolino 2017).

To combine the structural and equipment components, fragility curves can be converted into mean annual failure rates to match equipment data. One way to achieve this is to apply the theorem of total probability to calculate the yearly rate of failure $\left(v_f^{Yr}\right)$, by weighting the fragility by the probability of occurrence of the IM $\left(f(\mathrm{IM})\right)$ and integrating over IM:

$$v_f^{Yr} = \int G[DM|IM] \cdot f(IM) \cdot dIM \rightarrow \sum_{i=1} G[DM|IM_i] \cdot \left(\frac{1}{MRP_i} - \frac{1}{MRP_{i+1}}\right) \quad (3)$$

The $f(\mathrm{IM})$ term is evaluated by assuming that each MRP is related to a yearly probability of occurrence. The fragility curves are calculated using a limited sample of structural simulations, therefore are associated with uncertainty. The effect of this statistical error can be quantified by resampling the consequence metric (defined in the following section) using statistical bootstrapping.

3.5. Loss

An OWT system consists of different components each of which has two discrete states (failure or operation). For a system with a number (N) of independent components, there is a finite number of permutations in the system state, where the total number of combinations of component failure states is 2^N. These combinations of states can be summarized in a matrix K (e.g., Mensah and Dueñas-Osorio 2012), with elements $k_{ij} \in \mathbb{Z}^{N \cdot 2^N}$, using one to indicate that the component fails or zero to indicate that it remains operational. For a generic OWT with 11 components (Table 1), the matrix will be $k_{ij} \in \mathbb{Z}^{11 \cdot 2048}$. The first column will read $[0\ 0\ 0\ 0\ 0\ 0\ 0\ 0\ 0\ 0\ 0]^T$ indicating the case in which all components are functional, and the last $[1\ 1\ 1\ 1\ 1\ 1\ 1\ 1\ 1\ 1\ 1]^T$ indicating the case where all components have failed. Intermediate columns will contain all other permutations of ones and zeros for different system states. If each component has a deterministic material cost, then the discrete system failure events can be combined to assess the probability of incurring a repair cost (c_r). The matrix of the failure events K is converted into a failure cost matrix K_c by multiplying each column of K by a vector containing the failure cost of each component. This new matrix contains the same number of elements as K but the values will equal the failure cost as opposed to a logical value. Then $P_{sys}(c_r)$ can be defined as the probability a set of components fail $k^* \in K_c$ whose combined repair cost is equal the target (c_r):

$$P_{sys}(c_r) = \sum_{\boldsymbol{k}^* \in \boldsymbol{K_c}} \prod_{i=1}^{N} P_i^{k_i} (1 - P_i)^{1-k_i} \quad (4)$$

$P_{sys}\ (c_r)$ is evaluated over the columns of the K matrix where the total repair cost of the components equals c_r, i.e., k^* is a subset of K that contains all vectors of system status with equal cost. The probability of each combined repair cost is the product of the individual component failure probabilities in the matrix of failure events k^* as this calculation assumes each component is independent. When k_i is 0, then the probability that the component survives is used, i.e., $(1 - P_i)^{1-k_i}$; and if k_i is 1, then the probability that the component fails is used, i.e., $P_i^{k_i}$.

In Eq. (5), the overall consequence (Eq. (1); or total annual loss) is calculated by multiplying the yearly probability of different failure costs occurring $\left(P_{sys}(c_r)\right)$ by the consequence defined by direct material cost (c_r) and summing over all failure costs:

$$C(storms) = Loss_{total} = \sum_{c_r} P_{sys}(c_r) \cdot c_r \quad (5)$$

4. ILLUSTRATIVE APPLICATION

4.1. Case-study OWF

The OWF investigated in this paper is located at Ijmuiden K13, off the coast of the Netherlands and

has been previously used to generate fragility curves (Wilkie and Galasso 201X). The water depth at the site is around 20m, making it a suitable location for the NREL 5MW OWT on a monopile foundation. A full list of turbine dimensions and material properties are provided by (Jonkman et al. 2009). The structural components included in this study are the tower and blades, the replacement costs for these components are shown Table 1.

Data for the non-structural components of the considered OWT were taken from (Carroll et al. 2016). In this work, we focus on severe failures associated with major repairs, not on routine maintenance tasks. Only the 9 components with the highest failure rates in terms of major replacement cost (out of a total of 19 components) were used in this work and are shown on Table 1. Costs have been rounded to the nearest €1,000, improving computational efficiency in evaluating Eq. (5) numerically.

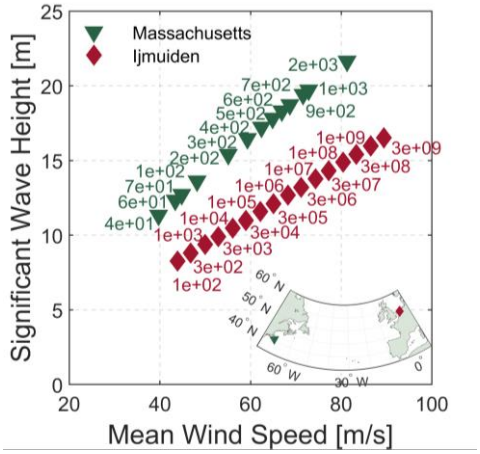

Figure 3. Comparison of the extreme wind and wave conditions associated with different MRP at Ijmuiden and Massachusetts OWF sites, inset map shows the location.

4.1.1. Structural failure cost

Total OWT cost (c_{WT}) in k€, including blades and drivetrain but excluding foundations, was estimated by (Dicorato et al. 2011) parameterized on the rated power of the turbine (P_{WT}) in megawatts (MW):

$$c_{WT} = 2.95 \cdot 10^3 \cdot ln(P_{WT}) - 375.2 \qquad (6)$$

Analysis by (Mone et al. 2015) reported that the cost of an onshore wind turbines tower comprised 17.6% of the total turbine cost. The cost of the OWT tower is calculated by factoring down the wind turbine cost to 17.6% of c_{WT}, assuming consistency in the relative cost between onshore and OWT components.

4.2. Hazard

Mean wind speeds and significant wave heights are plotted against their corresponding mean return period (MRP) in Figure 3; both are evaluated using site-measured data. A second set of data is shown for a site on the US East Coast, which has been assessed, but will not be presented in this paper due to space limitations. Full details of the hazard models for both sites are present (Wilkie and Galasso 201X).

Table 1: Material cost and failure rate for OWT sub-assemblies.[1] Eq. (6) with data – [$P_{WT} = 5MW$].

Cost source	Component	Major replacement [€]	Failure [/turbine/ year]
Carroll [32]	Gearbox	230,000	0.154
	Hub	95,000	0.001
	Transformer	70,000	0.001
	Generator	60,000	0.095
	Circuit breaker	14,000	0.002
	Power supply	13,000	0.005
	Pitch system	14,000	0.001
	Yaw system	13,000	0.001
	Controller	13,000	0.001
	Blades (x3)	270,000	2.32E-05
Equation	Tower	770,000[1]	8.36E-05
	Total cost	1,562,000	

4.3. Structural analysis model

Structural analysis was based on dynamic time-history simulation with integrated wind and wave loading. The structural limit states modelled in this case study use only the blades and tower, as previous work by the authors identified these as the critical structural components. The structure is assumed to work as a series system, the monopile and transition piece were observed to fail after the tower had reached 100% probability of failure. This indicates that the tower always fails first for the site assessed. The blades are assessed to

collapse when the blade root moment reaches a threshold maximum and the tower fails in buckling. Full details of the analysis methodology and the specifics of modelling stochastic wind and wave conditions are provided (Wilkie and Galasso 201X).

5. RESULTS AND DISCUSSION

5.1. Fragility curves

The fragility curves used in this study were, generated by selecting 16 MRP and running 400 structural simulations at each MRP to calculate the probability of failure (Wilkie and Galasso 201X). This analysis includes a set of random variables (referred to as X3 in the reference) which modelled variability in material properties, model uncertainty and orientation of the blades with respect to the incoming wind flow. The tower component is represented using a parametric lognormal fragility curve and the blade using an empirical fragility curve (as the lognormal assumption was found to provide a poor fit), shown in Figure 4.

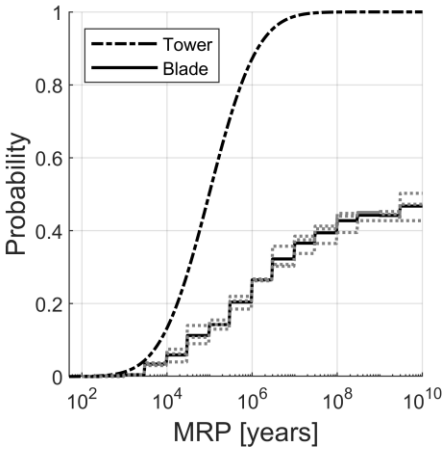

Figure 4. Fragility curves for the tower and blade. Grey lines indicate the empirical fragility curves for individual blades, the black line is the average.

Analysis in this paper uses statistical resampling to assess variability caused by using a reduced structural simulation size (as $400 \cdot 16 = 6400$ simulations are too computationally demanding for a practical application). New sets of fragility data are sampled, with replacement, from the original set of analysis results. The impact of statistical error can be evaluated by quantifying the scatter in the failure rate that results from scatter in the fragility curve parameters.

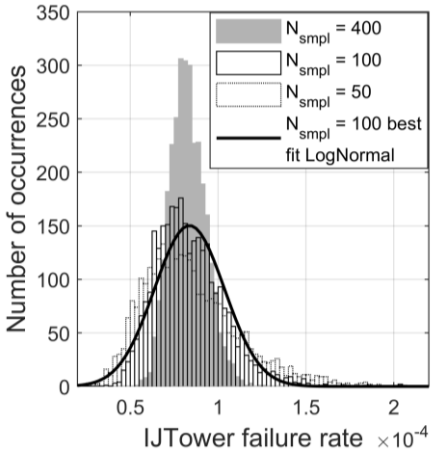

Figure 5. Histogram of failure rate for tower when different samples are used to fit a fragility function.

5.2. Structural component yearly failure rates

The integral in Eq. (4) is solved numerically, over the range of MRPs bounded by the limits $\mathrm{MRP_i} = [10, 10^6]$ and using a step size (dIM) of 1 year. The failure rate is evaluated using each of the resampled fragility curves, resulting in scatter – this is shown in Figure 5 for the tower, which is also representative of results for the blades. A lognormal PDF has been fitted to the histogram representing the case in which 100 samples are used. The scatter reduces as the number of samples increases, and the distribution fit to 100 samples used in remainder of this work. The mean failure rates of the tower and blades are presented on Table 1, calculated by taking the expectation over all samples.

5.3. Combined loss assessment

Loss estimation was initially implemented using the mean failure rates from Table 1. Blades are the main source of aero-dynamic loading and, if these fail, the loads on the tower will reduce. Consequently, the tower may not fail at high wind speeds. Conversely, if the blades survive but the tower collapses first, all equipment and the blades will fall into the sea and be damaged. To gain

insight into this, four assumptions relating to failure of the OWT components were tested:

- Case 1: Tower and other failures correlated – A new matrix K_1 (Section 3.5) is generated where failure of the tower results in the failure of all other components.
- Case 2: A new matrix K_2 (Section 3.5) is generated. Firstly, failure events that include the blades modified to prevent failure of the tower. Then the remaining cases where the tower fails (but the blades do not) cause failure of all other components.
- Case 3: Uncorrelated components, the K matrix left unchanged.
- Case 4: No structural failure, only equipment components fail, and empirical data from Table 1 is used.

These assumptions about the dependency of the OWT components are encoded into the loss calculation by creating an updated the matrix of failure events (K). The updated matrix is used to evaluate which subset of failure events are used $\boldsymbol{k}^* \in \boldsymbol{K_c}$ at each cost level in Eq. (4).

The annual loss complimentary CDF is presented in Figure 6, showing that low repair cost failures occur with relatively large probability and that these are driven by the more frequently occurring equipment failures. The method which excludes structural failures cannot predict repair costs above €1M, which include the tower. Using independent components results in a range of failure costs that involve the tower, whereas the correlated failure modes predicts a repair cost that is the sum of all equipment and tower costs, $1,562,000 (including the three blades). This is more accurate, as collapse of the tower will destroy all equipment in the hub. Small differences are visible in assumptions about blade, due to rarity of blade failure compared to the tower. This is explained by Eq. (4), as for each set of failure events the yearly probability of occurrence is the product of the probability of failures (components that fail) and probability of survival (components that survive). The gearbox and generator have high failure rates and therefore, failure events which do not include both are extremely rare.

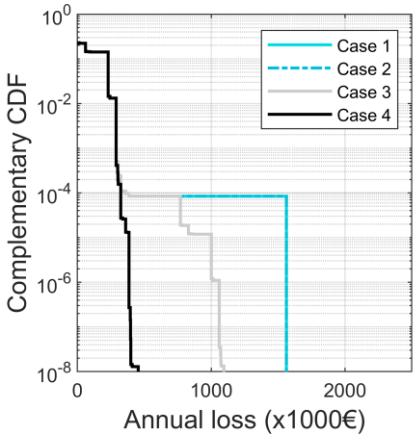

Figure 6. OWT loss CCDF comparing the four assumptions used in calculating loss.

5.4. System loss

Loss for the OWT is estimated using Eq. (5). Uncertainty in the structural failure rates can be included in the loss calculation by sampling the distributions describing failure rates of the blade and tower (i.e., Figure 5) and using the random samples as input to Eq. (4). The resulting empirical distribution of losses is shown in Figure 7. Again, little difference visible in the two cases where perfect correlation in the failure cases is assumed. The uncorrelated case is not conservative, because the average losses are lower. However, results for the Massachusetts site, mentioned in Section 4.2, show larger difference; failure rate of the blades is higher relative to the tower, and so preemptive failure of blades has a larger impact on losses. In this situation the average yearly losses in Case 2 are small in relation to Case 1. However, the presence of hurricane type conditions at the site make the overall losses much higher, and mean that the structural components play a more important role. These differences emphasize the need for a site-specific approach to the structural components of OWT. This calculation can be scaled to the OWF by multiplying the losses from a single OWT by the number of OWT in the farm, assuming that all act independently.

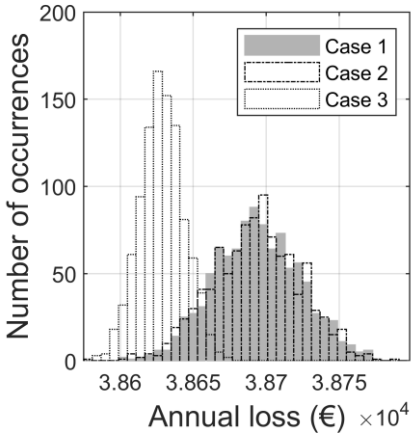

Figure 7. Histogram of loss for OWF when uncertainty in structural failure rates is modelled.

6. CONCLUSIONS

This paper introduced a method for estimating structural robustness of an OWT, as a first step towards quantifying resilience of OWF using a CAT framework to quantify economic losses due to extreme events. A case-study demonstrated how the calculation could be implemented to estimate losses associated with the important sub-systems of an OWT and scale loss to the OWF. The approach can be applied at the design stage, to test the impact of different design strategies on the OWF loss profile. Resilience is simplified to estimation of the consequence of OWT failure, defined in terms of repair cost alone. This allows the concept to be applied by practicing engineers who will not have access to the data required for a full evaluation of resilience, including potential recovery phases. As robustness is a component of resilience, the simplified method could be used as an input to a more comprehensive assessment.

7. ACKNOWLEDGEMENTS

This work was supported by the UK Engineering and Physical Sciences Research Council (EPSRC), DTP grant EP/M507970/1 for University College London. The authors acknowledge the use of the UCL Legion High Performance Computing Facility (Legion@UCL) and associated support services, in the completion of this work.

8. REFERENCES

Arwas, P., and Charlesworth, D. (2012). *Offshore wind cost reduction: pathways study*.

Bruneau, M., and Reinhorn, A. (2007). "Exploring the concept of seismic resilience for acute care facilities." *Earthquake Spectra*, 23(1), 41–62.

Carroll, J., McDonald, A., and McMillan, D. (2016). "Failure rate, repair time and unscheduled O&M cost analysis of offshore wind turbines." *Wind Energy*, 19(6), 1107–1119.

Dicorato, M., Forte, G., Pisani, M., and Trovato, M. (2011). "Guidelines for assessment of investment cost for offshore wind generation." *Renewable Energy*, Elsevier Ltd, 36(8).

Hosseini, S., Barker, K., and Ramirez-Marquez, J. E. (2016). "A review of definitions and measures of system resilience." *Reliability Engineering and System Safety*, 145, 47–61.

Iervolino, I. (2017). "Assessing uncertainty in estimation of seismic response for PBEE." *Earthquake Engineering & Structural Dynamics*, 46(February), 1711–1723.

Jonkman, J., Butterfield, S., Musial, W., and Scott, G. (2009). *Definition of a 5-MW reference wind turbine for offshore system development*.

Mensah, A. F., and Dueñas-Osorio, L. (2012). "A closed-form technique for the reliability and risk assessment of wind turbine systems." *Energies*, 5(6), 1734–1750.

Mone, C., Smith, A., Maples, B., and Hand, M. (2015). *2013 Cost of wind energy review; NREL/TP-5000-63267*.

Quiel, S. E., Marjanishvili, S. M., and Katz, B. P. (2015). "Performance-based framework for quantifying structural resilience to blast-induced damage." *Journal of Structural Engineering*, 142(8), C4015004.

Vorpahl, F., Schwarze, H., Fischer, T., Seidel, M., and Jonkman, J. (2013). "Offshore wind turbine environment, loads, simulation, and design." *Wiley Interdisciplinary Reviews: Energy and Environment*, 2(5), 548–570.

Wei, K., Arwade, S. R., and Myers, A. T. (2014). "Incremental wind-wave analysis of the structural capacity of offshore wind turbine support structures under extreme loading." *Engineering Structures*, Elsevier Ltd, 79, 58–69.

Wilkie, D., and Galasso, C. (n.d.). "Site-specific ultimate limit state fragility of offshore wind turbines on monopile substructures." *Engineering Structures [Under Review]*.